Thermochimica Acta, 96 (1985) 81–90
Elsevier Science Publishers B.V., Amsterdam – Printed in The Netherlands

INFLUENCE OF THE GRAIN MORPHOLOGY OF V_2O_5 ON ITS REDUCTION–REOXIDATION BEHAVIOUR

MAREK MACIEJEWSKI *, ARMIN RELLER and ALFONS BAIKER **

Swiss Federal Institute of Technology (ETH), Department of Industrial and Engineering Chemistry, CH-8092 Zürich (Switzerland)

(Received 4 June 1985)

ABSTRACT

The influence of the grain morphology of V_2O_5 on its reduction–reoxidation behaviour has been investigated by means of thermoanalytical methods, X-ray analysis and electron microscopy. Well-developed V_2O_5 platelets exposing predominantly the (010) face exhibited a significantly different reduction profile than poorly defined agglomerates of microcrystalline V_2O_5. Intermediate phases detected during reduction were V_6O_{13} and VO_2 (rutile). The corresponding reoxidation profiles were found to be only weakly dependent on the grain morphology of V_2O_3. Electron microscopy showed that the original grain morphology of the V_2O_5 samples was not influenced markedly by the reduction–reoxidation cycle.

INTRODUCTION

It is well known that in many oxidation reactions lattice oxygen plays an important role. Sachtler et al. [1] have shown that the rate at which the bond strength of the lattice oxygen increases with the degree of reduction influences the selectivity. Hence, the reduction characteristics of an oxidation catalyst can, at least in some cases, contribute to the understanding of its activity and selectivity behaviour. Vanadium pentoxide is a widely used catalyst for oxidation reactions [2]. It has been shown recently that the grain morphology, i.e., the distribution of the crystal planes exposed at the surface, can play an important role for the activity and selectivity of V_2O_5 in oxidation reactions. Gasior and Machej [3] reported that the selectivity of *o*-xylene oxidation to phthalic anhydride was correlated to the relative contribution of the (010) planes and, hence, to the amount of V=O bonds at the external surface. Recently, Baiker et al. [4] found that well-developed platelets of V_2O_5, with a large contribution of the (010) planes were about thirty times more active for CO oxidation than poorly defined agglomerates of needle-type V_2O_5, with comparably little contribution of these planes.

* On leave from Warsaw Technical University, 00-664 Warsaw, Poland.
** To whom correspondence should be addressed.

0040-6031/85/$03.30

Considerable effort has been expended to investigate the different intermediate oxide phases existing in the composition range V_2O_5 to V_2O_3 [5–11]. Some of them were found during reduction of V_2O_5 with hydrogen. Sata et al. [5,6] have found several new phases in the range V_6O_{13} to VO_2. Andersson [7] identified eight intermediate phases whose compositions can be expressed by the general formulae V_nO_{2n-1} ($n = 3, 4 \ldots 8$ and $n = \infty$) and V_nO_{2n+1} ($n = 6$). According to Hirotsu et al. [8], V_nO_{2n-1} (Magnéli phases) have a long period shear structure with triclinic symmetry. Theobald et al. [9] investigated the reduction of V_2O_5 to V_2O_3 by several gases and vapours and found that, depending on temperature, different intermediate vanadium oxides are formed. Kosugo [10] studied the phase relation in the V_2O_5–V_2O_3 system and the homogeneity range of each Magnéli phase by magnetic, X-ray and differential thermal analyses. Tilley and Hyde [11] found a number of new phases in their interesting transmission electron microscopy study of the decomposition of V_2O_5 in vacuum. More recently, Bosch et al. [12] investigated the reduction of V_2O_5 by means of temperature programmed reduction (TPR). They studied the influence of different factors, such as flow rate, heating rate, water partial pressure and sample weight, on the measured reduction profile.

Although considerable effort has been expended to investigate the different intermediate oxides existing in the composition range V_2O_5 to V_2O_3, to our knowledge, only very little is known about the influence of the grain morphology of V_2O_5 on its reduction–reoxidation behaviour. With this in mind, we have investigated the reduction–reoxidation behaviour of V_2O_5, focusing mainly on the influence of the grain morphology.

EXPERIMENTAL

Thermal analysis experiments were performed on a Mettler 2000C thermoanalyser. The conditions used for the reduction experiments were: heating rate, 5 K min^{-1}; hydrogen flow rate, 40 cm^3 min^{-1}; sample weight, 30–50 mg. Hydrogen was purified by passing it through a Deoxo-purifier (Engelhard) and a molecular sieve trap. A small, cylindrical Pt-cup of 8 mm diameter and 4 mm height was used as sample holder. Reoxidation experiments of the reduced samples were carried out under the same conditions but in air (40 cm^3 min^{-1}) instead of hydrogen.

X-ray analysis of the phases was performed on a Guinier IV-camera FR 552 with Johansson monochromator (Nonius, Delft) using Cu $K\alpha_1$ radiation.

Three samples of V_2O_5 with different grain morphology were used in our investigation. Sample A consisted of well-developed plate-like grains, with the large faces corresponding to (010) planes [13]. Samples B and C contained poorly defined agglomerates of needle-type grains. Sample A was obtained from ammonia metavanadate which was heated for 2 h at 700°C

and subsequently allowed to cool in the oven; B was commercially available V_2O_5 supplied by Fluka AG, Switzerland; C was obtained by isothermal decomposition of ammonia metavanadate at 470 K under vacuum (10 Pa). The BET surface area of the samples as measured by krypton adsorption at 77 K were: sample A, $0.32 + 0.02$ m^2 g^{-1}; sample B, $1.54 + 0.03$ m^2 g^{-1}; sample C, $91.2 + 0.5$ m^2 g^{-1}. Calculations were based on a cross-sectional area of 19.5 $Å^2$ for a krypton atom.

RESULTS

Reduction

The scanning electron micrographs presented in Fig. 1 illustrate the different grain morphologies of the V_2O_5 samples used in the experiments. The DTG and DTA curves recorded during reduction of the V_2O_5 samples in pure hydrogen are shown in Fig. 2. Note the differences of the samples in the reactivity (temperature of onset and completion of reduction, steepness of TG curve) and of the course of the reduction. The reduction of the V_2O_5 platelets (sample A) started at about 735 K and did not exhibit any intermediate step in the DTG and DTA curves. The reduction of sample B (needle-type agglomerates) started at slightly lower temperature and proceeded through three distinguishable steps, indicated by the minima in the DTG, or the maxima in the DTA curves at 813, 848 and 866 K. The weight loss (TG curve) at 813 K corresponds closely to the stoichiometric composition VO_2; the weight loss at 848 K corresponds to V_3O_5, and the one at 866 K to a composition between V_3O_5 and V_2O_3. The reduction of the microcrystalline high surface area V_2O_5 (sample C) started at considerably lower temperature, 523 K, and proceeded through two distinguishable steps with minima in the DTG curve at 728 and 756 K. The first step can be attributed to the reduction of V_2O_5 to VO_2 as X-ray analysis and the weight loss indicated.

For all three samples the final reduction products was pure V_2O_3 as evidenced by X-ray analysis. This result is supported by the agreement between calculated (17.6%) and measured weight losses for the samples during reduction of V_2O_5 to V_2O_3. Electron microscopy showed that the grain morphologies of the V_2O_3 samples resembled the corresponding grain morphologies of the original V_2O_5 samples, i.e., the grain morphologies were virtually restored during the reduction. The only change observed was a slight roughening of the grain surfaces.

In order to study the influence of a lowering of the hydrogen concentration on the reduction behaviour, we carried out measurements at lower hydrogen concentrations. For this purpose, part of the hydrogen stream was substituted by nitrogen. Figure 3 shows the thermoanalytical curves obtained

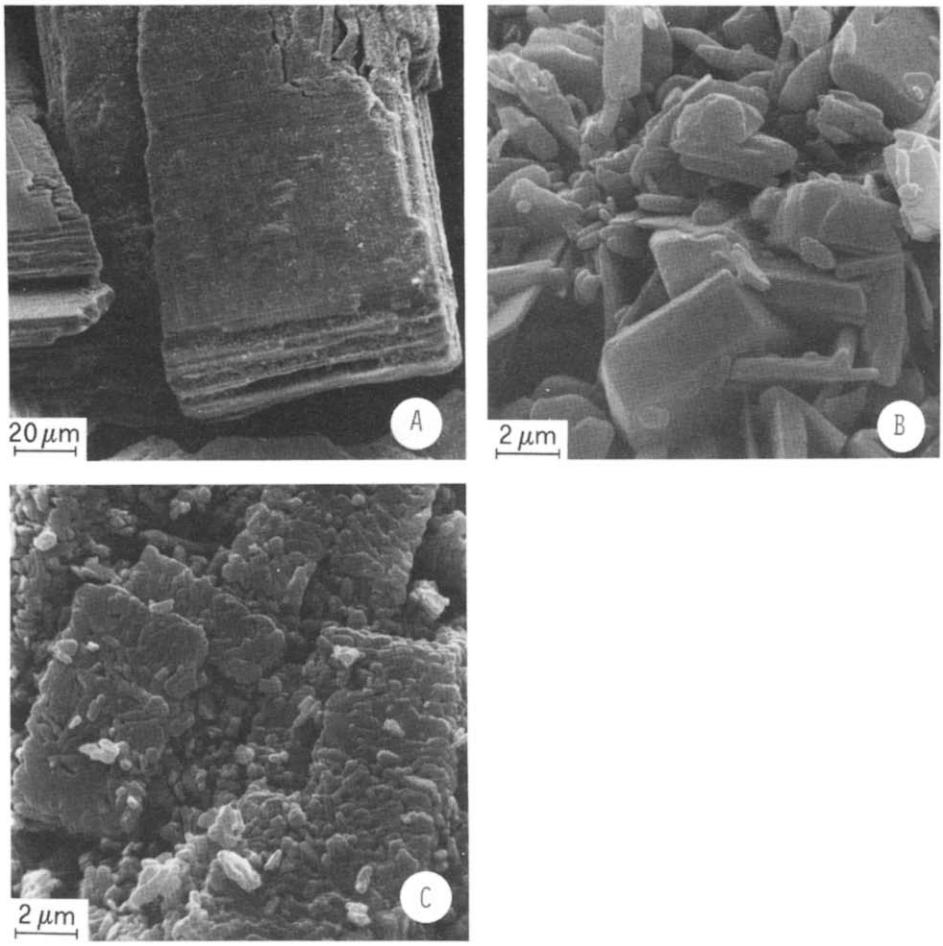

Fig. 1. Scanning electron micrographs of V_2O_5 samples. (A) V_2O_5 platelets grown from melt. (B) Microcrystalline V_2O_5 obtained by decomposition of NH_4VO_3 under non-isothermal conditions at atmospheric pressure. (C) Microcrystalline V_2O_5 obtained by decomposition of NH_4VO_3 under isothermal conditions (473 K) and reduced pressure (10 Pa).

with 10% hydrogen in nitrogen for sample B. A comparison of the results of this measurement with those obtained with pure hydrogen (Fig. 2B) indicates that lowering of the hydrogen concentration had three main consequences: (i) four peaks corresponding to different reduction steps are distinguishable in the DTG curve; (ii) the reduction rate decreases and the reduction profile is shifted to higher temperature; (iii) two endothermic peaks occur in the DTA curve, the first at 956 K, the second at 988 K. These peaks are attributed to partial melting of some phases during reduction. Likely candidates for phases thermally unstable in this temperature range are V_2O_5, V_3O_7 and V_6O_{13}. Figure 4 depicts the influence of these sintering and melting

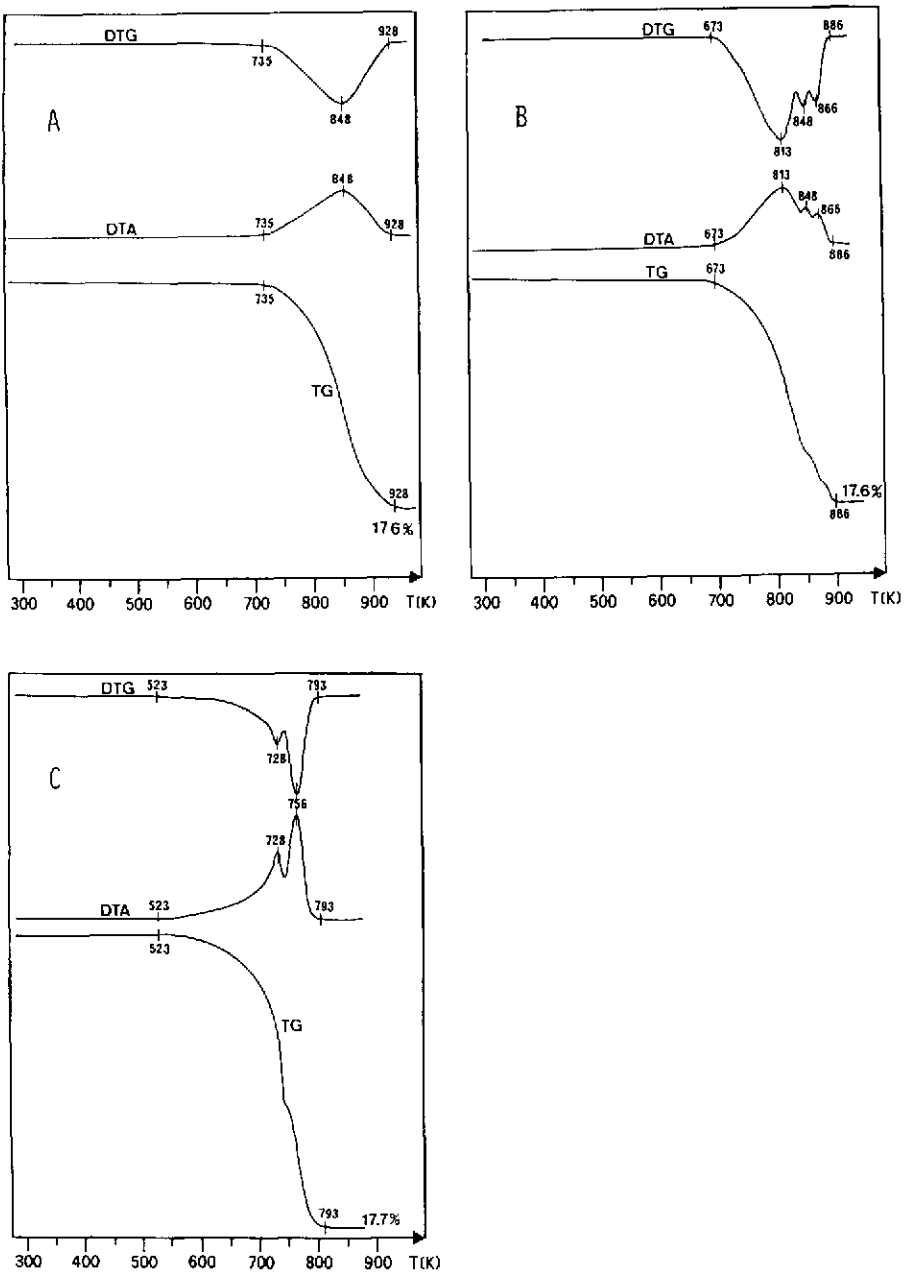

Fig. 2. Combined TG–DTG–DTA measurements of the reduction of V_2O_5 samples in pure hydrogen. Grain morphologies of samples are shown in Fig. 1. Conditions: heating rate, 5 K min^{-1}; hydrogen flow rate, 40 cm^3 min^{-1}; sample weights: (A) 43.1 mg; (B) 43.1 mg; (C) 56.4 mg. Theoretical weight loss, 17.6%.

processes on the grain morphology. As outlined above, reduction with pure hydrogen did not lead to significant changes of the original grain morphology.

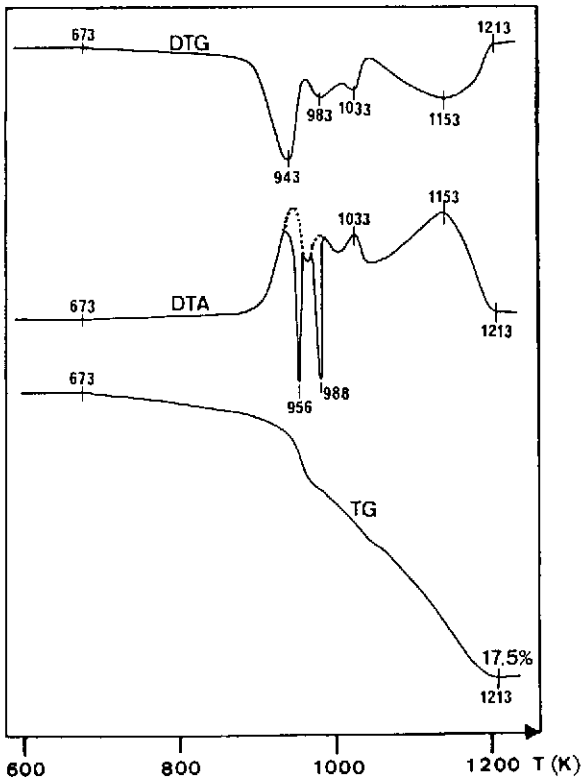

Fig. 3. Combined TG–DTG–DTA measurements of the reduction of V_2O_5 (B) in a mixture of 10% hydrogen and 90% nitrogen. Conditions: heating rate, 5 K min^{-1}; total flow rate, 40 cm^3 min^{-1}; sample weight, 43.3 mg.

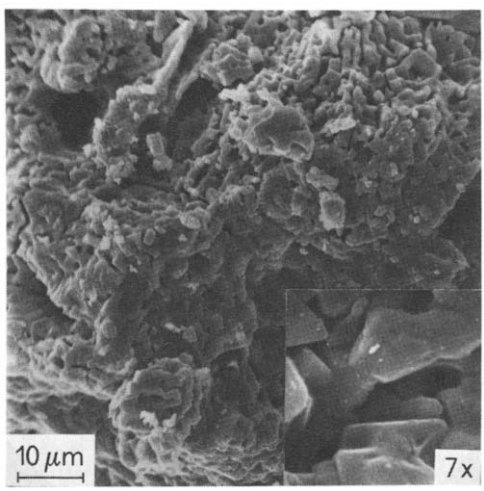

Fig. 4. Scanning electron micrograph of V_2O_3 obtained by reduction of V_2O_5 (B) in a mixture of 10% hydrogen and 90% nitrogen. Inset at the lower right corner shows a magnified section of the sintered product V_2O_3. Thermoanalytical curves and conditions of reductions are shown in Fig. 3.

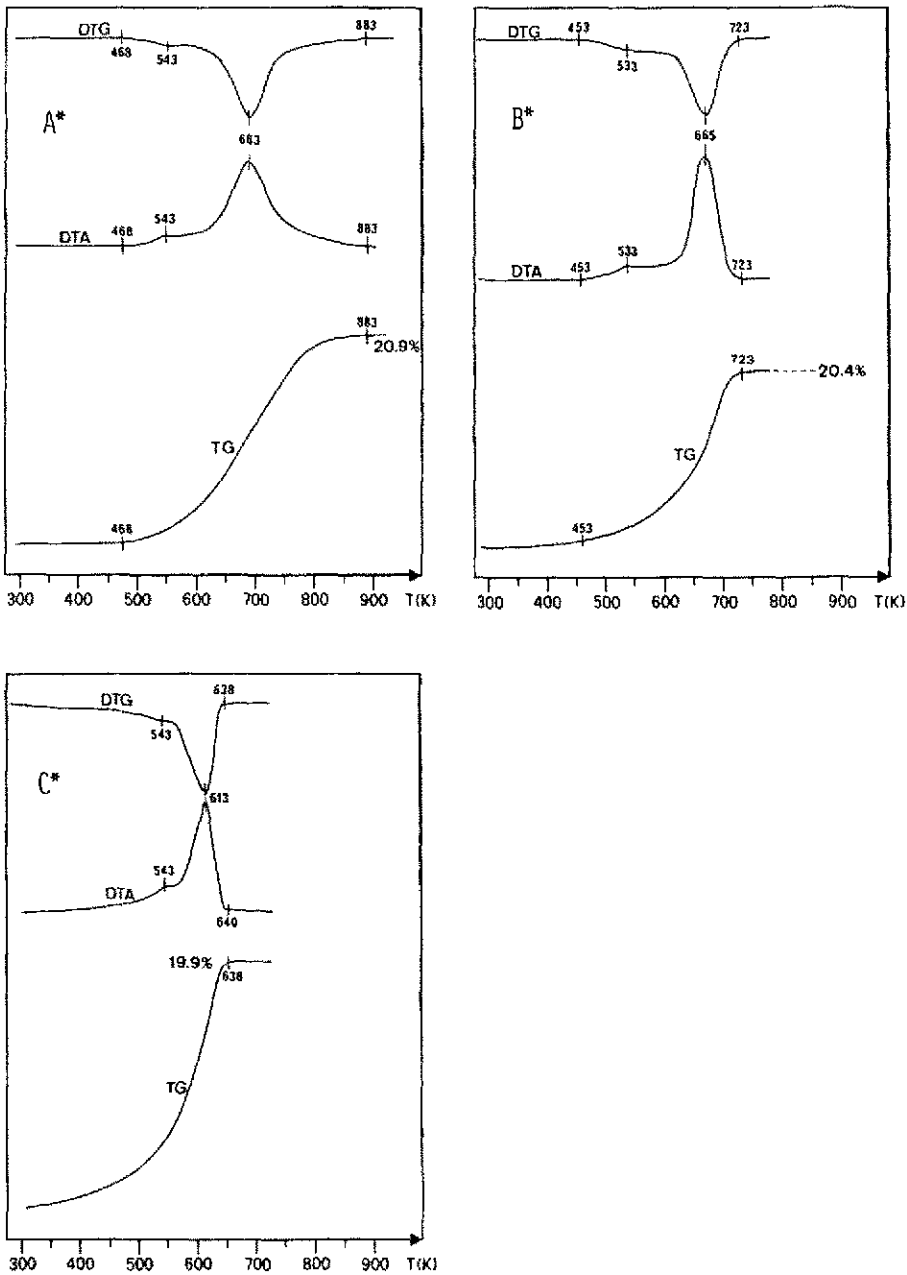

Fig. 5. Combined TG–DTG–DTA measurements of the reoxidation of V_2O_3 to V_2O_5 in air. (A*) sample obtained by reduction of A (see Figs. 1 and 2); (B*) sample obtained by reduction of B; (C*) sample obtained by reduction of C. Conditions: heating rate, 5 K min^{-1}; air flow rate, 40 cm^3 min^{-1}. Sample weights: (A*) 33.9 mg; (B*) 33.3 mg; (C*) 41.3 mg. Theoretical weight gain, 21.35%.

Reoxidation

Reoxidation of the V_2O_3 samples obtained by reduction in pure hydrogen (Fig. 2) was performed in air (40 cm^3 min^{-1}) at a heating rate of 5 K min^{-1}. The results of these thermoanalytical measurements are presented in Fig. 5. For all V_2O_3 samples the DTG and DTA curves exhibited two distinguishable steps and the increase in weight was slightly less than the calculated stoichiometric value (21.3%) for the oxidation of V_2O_3 to V_2O_5. The latter phenomenon is attributed to some oxygen uptake at low temperature, i.e., before the start of the measurement. However, it should be noted that the reactivity of the V_2O_3 towards oxygen is considerably different. The highest reactivity is exhibited by sample C* (reduced form of sample C) for which oxidation started at about 320 K and was finished at 638 K. Sample A* exhibited the lowest reactivity, reoxidation started at 470 K and was completed at 880 K. Although the onset of reoxidation of sample B* occurred at slightly higher temperature than the one of sample A*, the reoxidation proceeded much faster on this sample, which is indicated by the considerably steeper TG curve. The resulting products of all three samples were pure V_2O_5, and the grain morphologies resembled those of the corresponding original samples. This was evidenced by X-ray analysis and electron microscopy.

DISCUSSION

Our comparative study using thermoanalysis, X-ray diffraction and scanning electron microscopy indicates that the grain morphology of V_2O_5 is a decisive factor influencing the course of the reduction of V_2O_5 to V_2O_3. This is substantiated by the reduction profiles (DTG, DTA, TG curves) of V_2O_5 samples of different grain morphology compared in Fig. 2. When comparing these curves, we have, of course, to take into account the large surface area of the microcrystalline V_2O_5 (C) as compared to the small surface areas of samples A and B. In this light, the much higher reactivity of C is not surprising. The thermoanalytical results indicate that during reduction one has to cope with a rather complicated sequence of overlapping and competing processes. It has to be considered that within reacting crystallites relatively high internal partial pressures of the product gas H_2O are built up, which leads to a decrease of the reduction rate and, depending on the actual sizes of the crystallites, one has to assume that several intermediate phases may be simultaneously present in such a way that there is a gradient of oxygen between the surface and the centre of the reacting material. Accordingly, no distinct plateaus can be registered by thermogravimetric measurements. This effect proves to be most prominent for the reduction of the well-developed V_2O_5 platelets (sample A) with comparatively large dimen-

sions. In line with this, the reduction of the microcrystalline materials (samples B and C) leads to the formation of several distinct intermediates VO_x reflected in the reduction profiles. Intermediate phases identified by X-ray analysis during the reductions shown in Fig. 2 were V_6O_{13} and VO_2 (rutile). This is in agreement with earlier investigations by Theobald et al. [9] and Bosch et al. [12]. Theobald et al. found V_6O_{13} and VO_2 (rutile) as intermediate phases during reduction of V_2O_5 at temperatures higher than 770 K. The same intermediate phases were also identified by Bosch et al. in their TPR experiments.

The concentration of the reducing agent H_2 within the ambient atmosphere proves also to be a decisive factor for the course of the reduction. This emerges from a comparison of the reduction profiles obtained for sample B in pure hydrogen (Fig. 2B) and in a mixture of 10% H_2 in nitrogen (Fig. 3). In the diluted system the reduction rate is considerably lower and the onset of reduction is shifted to a much higher temperature. As a result of this, sintering and partial melting of thermally unstable phases takes place. There are three solid phases in the system V_2O_5–V_2O_3 which are unstable in the temperature range of reduction: V_2O_5, V_3O_7 and V_6O_{13}. V_6O_{13} is stable only below 981 K, at this temperature it congruently melts into solid VO_2 and liquid. The V_3O_7 phase also has a peritectic temperature (953 K) at which it congruently melts into solid V_6O_{13} and liquid [10]. The measured endothermic peaks (Fig. 3) at 956 and 988 K are attributed to partial melting of V_2O_5 and V_6O_{13}, respectively. This observation has an important consequence for the characterization of vanadium oxide systems by means of temperature programmed reduction (TPR). In order to obtain optimal resolution of the reduction profiles, measurements are generally performed with low concentration (< 10%) of hydrogen in the carrier gas [12,14]. The DTA curve shown in Fig. 3 and the electron micrograph of the reduced sample (Fig. 4) indicate that TPR measurements performed with hydrogen concentrations lower than 10% are likely to be affected by superimposed melting processes. In fact, this is probably true for most TPR profiles of V_2O_5 reported previously [12,15,16].

The influences of the grain morphology on the onset temperature of fully reduced V_2O_5, i.e., of V_2O_3, are comparatively small. This behaviour cannot be attributed to smaller differences of the grain morphology of the V_2O_3 samples as compared to the original V_2O_5 samples. Electron microscopy showed that for all samples the grain morphology changed only very little (slight roughening of surface) during reduction, i.e., the V_2O_3 samples exhibited a grain morphology similar to the original V_2O_5 samples. The similarity of the shape of the reoxidation curves may be an indication that the course of the reoxidation is characterized by direct formation of the thermodynamically stable product phase at the surface and by a subsequent growth of the product phase into the initial V_2O_3 crystallites. It is likely that after an initial period, the diffusion of oxygen through the formed product

layer of V_2O_5 becomes the rate-determining step of the reoxidation process and governs the reoxidation profile. Finally, it is interesting to note that the grain morphology of the V_2O_5 samples after the reduction–reoxidation cycle was almost identical to that of the corresponding original V_2O_5 samples, i.e., it did not change markedly during the reduction–reoxidation cycle. This behaviour is important for possible regeneration of V_2O_5 used as catalyst.

CONCLUSIONS

Thermoanalytical measurements indicate that the reduction of V_2O_5 in a hydrogen atmosphere is strongly influenced by the grain morphology of the vanadium oxide. Depending on the grain morphology different intermediate steps are discernible in the reduction profiles. Lowering of the hydrogen concentration by dilution with nitrogen leads to a drastic decrease of the reduction rate and a shift of the onset of reduction to a higher temperature. As a result of this, superimposed partial melting processes occur which influence the course of reduction. In contrast to the reduction, the reoxidation shows only little dependence on the grain morphology. The grain morphology of V_2O_5 exhibits no significant change after the reduction–reoxidation cycle.

ACKNOWLEDGEMENT

We are grateful to the Swiss National Science Foundation for supporting this work.

REFERENCES

1 W.H.M. Sachtler, G.J.W. Dorgelo, J. Fahrenfort and R.J.H. Voorhoeve, Proc. 4th Int. Congr. Catal., Vol. I, Adademai Kiado, Budapest, 1971, p. 454.
2 D. Dadyburjor, S.S. Jewur and E. Ruckenstein, Catal. Rev. Sci. Eng., 19 (1979) 293.
3 M. Gasior and T. Machej, J. Catal., 83 (1983) 472.
4 A. Baiker, P. Dollenmeier and H. Renjin, J. Chem. Soc., Chem. Commun., 7 (1985) 413.
5 T. Sata, E. Komada and Y. Ito, Kogyo Kagaku Zasshi, 71 (1968) 643.
6 T. Sata and Y. Ito, Kogyo Kagaku Zasshi, 71 (1968) 647.
7 G. Andersson, Acta Chem. Scand., 8 (1954) 1599.
8 Y. Hirotsu, H. Sato and S. Nagakura, in J.M. Cowley et al. (Eds.), Conference Modulated Structures, American Institute of Physics, New York, 1979, p. 75.
9 F. Theobald, R. Cabala and J. Bernard, J. Solid-State Chem., 17 (1976) 431.
10 K. Kosugo, J. Phys. Chem. Solids, 28 (1967) 1613.
11 R.J.D. Tilley and B.G. Hyde, J. Phys. Chem. Solids, 31 (1970) 1613.
12 H. Bosch, B.J. Kip, J.G. Van Ommen and P.J. Gellings, J. Chem. Soc., Faraday Trans. 1, 80 (1984) 2479.
13 A. Bystrom, K.A. Wilhelmi and O. Brötzen, Acta Chem. Scand., 4 (1950) 1119.
14 D.M.A. Monti and A. Baiker, J. Catal., 83 (1983) 323.
15 A. Baiker and W. Zollinger, Appl. Catal., 10 (1984) 231.
16 A. Baiker and D.M.A. Monti, J. Catal., 91 (1985) 361.